DOI:10.1002/anie.201801202

Structural Basis of Outstanding Multivalent Effects in Jack bean α-Mannosidase Inhibition

Eduardo Howard,‡[a,d] Alexandra Cousido-Siah,‡[a] Mathieu L. Lepage,[b] Jérémy P. Schneider,[b] Anne Bodlenner,[b] André Mitschler,[a] Alessandra Meli,[c] Irene Izzo,[c] Ariel Alvarez,[d] Alberto Podjarny,[a] Philippe Compain*[b]

[a] A. Cousido-Siah, Dr. A. Mitschler, Dr. A. Podjarny
Department of Integrative Biology, Institut de Génétique et de Biologie Moléculaire et Cellulaire, CNRS, INSERM, UdS, 1 rue Laurent Fries, 67404 Illkirch CEDEX (France)

[b] Dr. M. L. Lepage, Dr. J. P. Schneider, Dr. A. Bodlenner, Prof. P. Compain
Laboratoire d'Innovation Moléculaire et Applications
Univ. de Strasbourg | Univ. de Haute-Alsace | CNRS | LIMA (UMR 7042)
Equipe de Synthèse Organique et Molécules Bioactives (SYBIO), ECPM
25 Rue Becquerel, 67000 Strasbourg, France
E-mail: philippe.compain@unistra.fr

[c] Prof. I. Izzo, Dr. A. Meli
Department of Chemistry and Biology "A. Zambelli"
University of Salerno
Via Giovanni Paolo II,132, 84084 Fisciano,Salerno (Italy)

[d] Dr. E. Howard, Dr. A. Alvarez
Instituto de Física de Líquidos y Sistemas Biológicos, CONICET, ULNP, Calle 59 No. 789, La Plata, Argentine

‡ These authors contributed equally to these work.

DOI:10.1002/anie.201801202

Abstract: *Multivalent design of glycosidase inhibitors is a promising strategy for the treatment of diseases involving enzymatic hydrolysis of glycosidic bonds in carbohydrates. An essential prerequisite for successful applications is the atomic level understanding of how outstanding binding enhancements are actually achieved with multivalent inhibitors. Here we report the first high resolution crystal structures of the Jack bean α-mannosidase (JBα-man) in apo and inhibited states. The three-dimensional structure of JBα-man in complex with the multimeric cyclopeptoid-based inhibitor displaying the largest binding enhancements reported so far provides decisive insights into the molecular mechanisms underlying multivalent effects in glycosidase inhibition.*

The modulation of the multiple biological activities of glycosidases is a major target for drug discovery.[1] Catalytic hydrolysis of glycosidic linkages, the most stable covalent single bonds within biopolymers, is indeed a fundamental process involved in key cellular events including energy uptake and post-translational modifications of glycoproteins.[2] Multivalent design of glycosidase inhibitors has recently experienced a major take-off with the disclosing of glycomimetic clusters showing outstanding affinity enhancements over the corresponding monovalent ligands (up to five orders of magnitude).[3-7] Although intensive efforts have been performed to rationalize the inhibitory multivalent effect observed, structural information into the way multimeric inhibitors and glycosidases interact at the atomic level remains unknown.[6] Recent studies in the field have logically focused on Jack bean α-mannosidase (JBα-man) since this high-molecular-weight (220 kDa) zinc-enzyme,[8] is the most sensitive to multivalent binding known to date.[6] JBα-man is a member of the retaining glycoside hydrolase family 38 (GH38) that contains therapeutically relevant α-mannosidases.[8] These mammalian enzymes participate to the biosynthesis and catabolism of *N*-glycan in cells[8b] and as such constitute targets for the treatment of cancers and lysosomal diseases.[9] In the absence of 3D crystallographic structure for JBα-man, interactions with multivalent inhibitors have been studied using indirect methods such as atomic force microscopy, dynamic light scattering, NMR or mass spectroscopy.[5-7] These studies have led to a number of competing hypotheses and binding models involving large aggregates, additional interactions with enzyme subsites or formation of discrete cross-linked complexes.[5-7] Here we report the first high-resolution crystal structures of apo JBα-man and of its complex with the 36-valent cluster **1**[7] (Figure 1). The experimental observation of multivalent interactions associated with molecular modelling suggests a clear rational basis for the outstanding affinity enhancement observed.

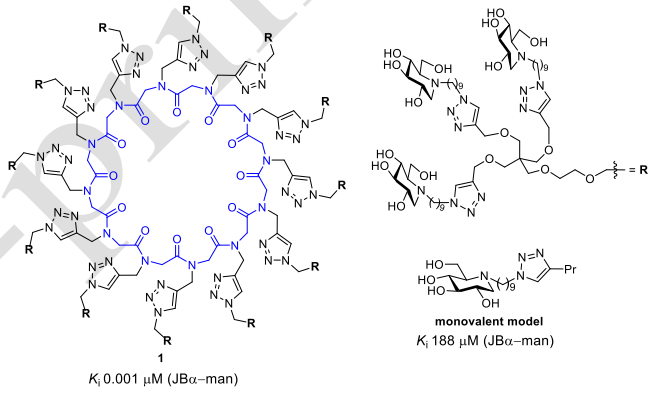

Figure 1. Mono- and 36-valent inhibitors of JBα-man. Pr = propyl.

The apo structure of JBα-man was solved by X-ray protein crystallography at 1.84 Å resolution (Protein Data Bank -PDB- entry 6B9O). Molecular replacement with Bovine Lysosomal α-Mannosidase (PDB entry 1O7D)[10] was successfully used for the initial structure determination. This protein was chosen following a sequence alignment of the published sequence for JBα-man[8a] against the full PDB content, which gave 40% identity (Tables SI1 and Figure SI1 in the Supporting Information). The crystallographic asymmetric unit has one JBα-man protein composed by two LH heterodimers, each formed by the two distinct chains, L1 and H1 (L:Light chain and H:Heavy chain) (Figure 2). This figure shows also the symmetry related $(LH)_2$ complex (LH1a and LH2a). The four active sites, identified by the zinc ions in the H-chain, are turned toward a cavity at the center of the complex composed by the four LH heterodimers. We anticipated that this large pocket could fit the size of large multivalent inhibitors such as **1**.

DOI:10.1002/anie.201801202

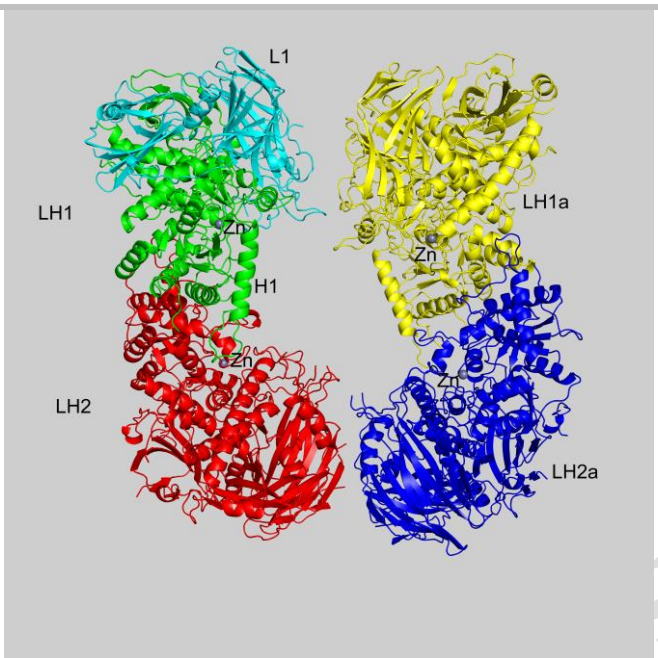

Figure 2. Ribbon representation of two $(LH)_2$ complexes, one formed by LH1 (L1 in cyan and H1 in green) and LH2 (in red) and a symmetry related one formed by LH1a (in yellow) and LH2a (in blue), and zinc atoms (grey sphere).

How JBα-man binds multimeric inhibitors is key to our analysis of the outstanding multivalent effects observed. To gain detailed insights at the atomic level, we attempted to determine the structures of complexes of JBα-man with diverse cyclopeptoid-based iminosugar clusters.[7] Extensive co-crystallization of enzyme:inhibitor complex was carried out by a Mosquito robot using sitting-drop vapor-diffusion method. Remarkably, well-diffracting crystals were obtained with **1** which displays the largest binding enhancement observed so far for a glycosidase (Figure 1).[7] The 36-valent cluster **1** complex structure of JBα-man was solved by X-ray protein crystallography at 2.0 Å resolution (PDB entry 6B9P). The overall structure of this complex was similar to the apo form of JBα-man with the same crystal parameters (space group and cell dimensions), indicating that multivalent inhibitor binding does not perturb the protein. The X-ray complex structure showed the mode of binding of four iminosugar heads of the 36-valent cluster **1** in the catalytic site of each LH heterodimer. In the X-ray structure, only one iminosugar head was clearly visible for each LH heterodimer in the electron density map at 2.0 Å resolution, suggesting the absence of a secondary binding site (Figure 3 and Figure SI2 in the Supporting Information). Non-specific interactions at the surface of the enzyme can, however, not be excluded. The iminosugar head of the multivalent inhibitor is buried in the catalytic pocket in the H-chain, while the aliphatic linker makes hydrophobic contacts with the protein surface (Figure 3 and Figures SI2-6 in the Supporting Information).

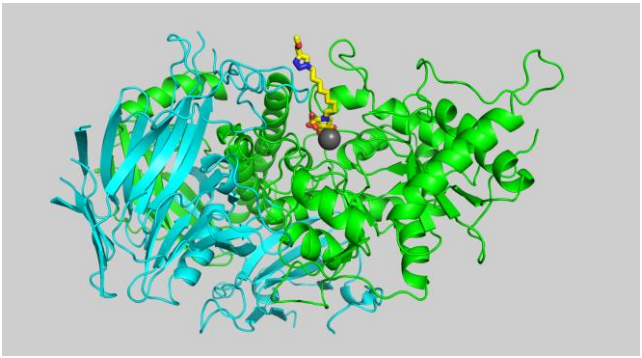

Figure 3. JBα-man protein structure in complex with iminosugar head and the aliphatic chain of **1**; cyan ribbon L-chain, green ribbon H-chain, yellow sticks carbon atoms, red sticks oxygen atoms, blue sticks nitrogen atoms and zinc atom grey sphere.

DOI:10.1002/anie.201801202

The zinc atom in the H-chain is clearly observed in an octahedric coordination with six atoms at distances between 2.1 Å and 2.3 Å (Figure 4); four oxygen atoms, two of them provided by protein aspartate residues (Asp^{145}, Asp^{25}) and two by the iminosugar head, and two nitrogen atoms provided by protein histidine residues (His^{23} and His^{386}). The geometry and the intervening residues are the same than in previously reported structures from two other proteins of the same GH38 family (Figure SI7 in the Supporting Information),[10-11] with the notable difference that the ligand in those previous structures provides only one zinc coordinating oxygen. The residue Asp^{145} is characteristic of GH38 α-mannosidases and has been demonstrated as the catalytic nucleophile in JBα-man.[12] Based on the expected distance (~ 5.5 Å) between the two catalytic carboxylate groups in retaining hydrolysis mechanism,[13] Asp^{25} would seem the most likely candidate for the catalytic acid/base (Figure SI6 in the Supporting Information). In addition, the involvement of the two catalytic residues in the coordination of the zinc ion is believed to be essential to the mechanism of the catalytic glycosidic cleavage.[10-11]

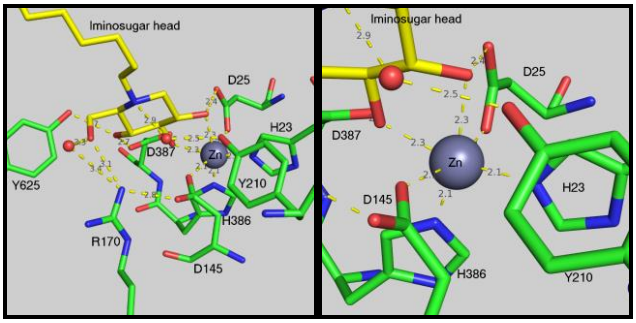

Figure 4: Contacts of iminosugar head with protein and zinc atom. Protein in green sticks, **1** in yellow sticks, zinc atom grey sphere and two water molecules red sphere. Left: Full site. Right: Zoom on Zn coordination.

No electron density could be observed beyond the quaternary carbon branching point of the trivalent dendron of cluster **1**. Since the considerable conformational flexibility of the cyclic peptoid core and associated ethylene glycol spacers precludes *a priori* direct information from X-ray crystallography, a 3D model of the full 36-valent cluster **1** was built and was successfully fitted into the cavity with the program Coot[14] (Figure SI8 in the Supporting Information). The iminosugar heads were kept in the positions shown in the X-Ray maps, the inhibitor core in the middle of the cavity and the remaining part between the core and the iminosugar heads in an arbitrary conformation. This encouraging result indicated that our binding model was sterically plausible. However, the absence of any signal corresponding to the disordered center of **1** in the electron density map at 2.0 Å prompted us to develop a convenient method to obtain experimental evidence for its location. A combination of symmetry lowering and low resolution maps eventually enabled us to observe a signal corresponding to the inhibitor core. Since the cavity spans two asymmetric units in $P2_12_12_1$, with one half of the cavity in each asymmetric unit, the disordered multivalent ligand might not respect the symmetry between both halves. In order to recover any diffraction signal, the whole cavity should be in a single asymmetric unit. To do this, the symmetry of both crystals (apo and holo) was reduced from orthorhombic ($P2_12_12_1$) to monoclinic ($P2_1$), expanding the asymmetric unit to include the two $(LH)_2$ complexes. The corresponding structure factors were recalculated from the raw images to recover all the information present in the diffraction data. The corresponding models (apo and holo) were placed in the $P2_1$ space group and re-refined, giving a very similar result to the $P2_12_12_1$ refinement for the protein. Maps were calculated in this new space group. As no high resolution details are expected, due to the flexibility of the multivalent ligand, map resolution was reduced from 2.0 Å to 5.0 Å, a suitable limit to enhance features of this size even with partial disorder. Electron density maps for the protein were very similar (Figure 5). However, a signal was observed at the center of the cavity only for the data from the crystal with the multivalent ligand **1**, strongly suggesting the presence of its core.

DOI:10.1002/anie.201801202

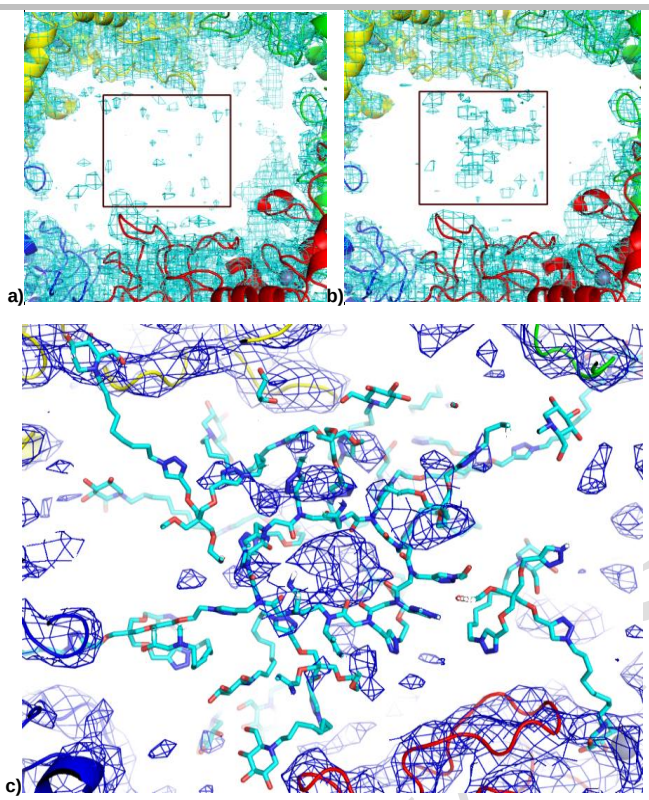

Figure 5: Electron density low resolution 2Fo-Fc map in blue (5 Å, 1.0 σ contour) and protein cartoon (yellow, blue, green and red). a) apo crystal; b) crystal with **1**; c) Close up on the density at the center superposed with the model of cluster **1** (cyan).

The conformational space of the multivalent ligand inside the cavity was explored with simulated annealing using the program Phenix,[15] starting from five different positions (generated manually with Coot[14]) for the linker arms and central core (Figure SI9 in the Supporting Information). In each of the five positions the same four heads were kept in the corresponding catalytic pockets. This led to five models clearly demonstrating that the four bound iminosugar heads belong to the same multivalent ligand. The observation of an electron density signal at the center of the cavity provides the experimental proof that this topology is the most probable one (Figure 5). The present structural study confirms the formation of a 2:1 JBα-man:inhibitor sandwich-type complex that was initially postulated on the basis of electron microscopy imaging, analytical ultracentrifugation measurements and mass spectroscopy experiments.[7]

The experimental observation of multivalent interactions associated with molecular modelling suggests a clear rational basis for the high affinity enhancements observed in JBα-man inhibition. In the binding topology proposed, the multivalent ligand occupies the cavity created by two $(LH)_2$ complexes, with the core placed at the center of this cavity, radial arms pointing towards the four catalytic sites present in the H subunits and four iminosugar heads binding to them. The bridging of two $(LH)_2$ complexes by four iminosugar heads of the multimeric inhibitor results in a strong chelation effect explaining the exceptionally large affinity enhancements observed.[7] The chelation effect is indeed considered to be the mode of binding underlying the most powerful multivalent effects reported to date.[16] It is noteworthy that inhibitor **1** fully occupies the cavity. Reduced multivalent effects may be anticipated for smaller clusters able to embrace only two catalytic sites simultaneously, or for giant clusters that would not fit inside the cavity, leading to other binding modes.[4f-g,7] The iminosugars that are not buried in the catalytic pocket remain in close proximity, opening the possibility of multiple bind-and-recapture processes.[17]

In conclusion, the first high-resolution crystal structures of apo JBα-man and of its complex with the 36-valent cluster **1** considerable insights at the atomic level into the way a glycosidase and a multimeric inhibitor interact to produce outstanding inhibitory multivalent effects. The X-ray crystallographic structure showed four ordered iminosugar heads of the 36-valent cluster **1** simultaneously engaging all four active sites of two JBα-man molecules to form a strong sandwich chelate complex. The crystal structures presented

here provide the foundations for a rational design of multivalent inhibitors targeting JBα-man and the related clinically relevant GH38 α-mannosidases.

Acknowledgements

X-ray data collection was performed on the PXIII beamline at the Swiss Light Source synchrotron, P. Scherrer Institute, Villigen, Switzerland. We thank V. Olieric and F. Dworkowski for their help on the beamline. We also thank the IGBMC structural platform staff, in particular P. Poussin-Courmontagne and A. Mc Ewen. This work has been funded by the CNRS, the INSERM, the Université de Strasbourg (IDEX program R701/W15RPE19), the Centre International de Recherche aux Frontières de la Chimie (FRC), the Région Alsace, the Hôpital Civil de Strasbourg, Instruct (part of the European Strategy Forum of Research Infrastructures; ESFRI), the French Infrastructure for Integrated Structural Biology (FRISBI), ANR-10-INSB-05-01 and a doctoral fellowship from the French Department of Research to MLL. We thank also the University of Salerno (FARB) and the Italian MIUR (PRIN20109Z2XRJ_006) for financial support.

Keywords: • cyclic peptoids • iminosugars • multivalency • hydrolases • X-ray diffraction

[1] a) V. H. Lillelund, H. H. Jensen, X. Liang, M. Bols, *Chem. Rev.* **2002**, *102*, 515-553. b) N. F. Bras, N. M. Cerqueira, M. J. Ramos, P. A. Fernandes, *Expert Opin. Ther. Pat.* **2014**, *24*, 857-874. c) P. Compain, O. R. Martin, *Iminosugars: from Synthesis to Therapeutic Applications* Wiley & Sons, Chichester, **2007**. d) R. J. Nash, A. Kato, C.-Y. Yu, G. W. Fleet, *Future Med. Chem.* **2011**, *3*, 1513-1521.

[2] a) N. Asano, *Glycobiology* **2003**, *13*, 93R-104R. b) W. W. Kallemeijn, M. D. Witte, T. Wennekes, J. M. F. G. Aerts, *Adv. Carbohydr. Chem. Biochem.* **2014**, *71*, 297-338.

[3] P. Compain, C. Decroocq, J. Iehl, M. Holler, D. Hazelard, T. Mena Barragán, C. Ortiz Mellet, J.-F. Nierengarten, *Angew. Chem. Int. Ed.* **2010**, *49*, 5753-5756.

[4] For selected references see: a) C. Decroocq, D. Rodríguez-Lucena, V. Russo, T. Mena Barragán, C. Ortiz Mellet, P. Compain, *Chem. Eur. J.* **2011**, *17*, 13825-13831; b) C. Bonduelle, J. Huang, T. Mena-Barragán, C. Ortiz Mellet, C. Decroocq, E. Etamé, A. Heise, P. Compain, S. Lecommandoux, *Chem. Commun.* **2014**, *50,* 3350-3352; c) A. Hottin, D. W. Wright, E. Moreno-Clavijo, A. J. Moreno-Vargas, G. J. Davies, J.-B. Behr, *Org. Biomol. Chem.* **2016**, *14*, 4718-4727. d) D. Alvarez-Dorta, D. T. King,T. Legigan, D. Ide, I. Adachi, D. Deniaud, J. Désiré, A. Kato, D. Vocadlo, S. G. Gouin, Y. Blériot, *Chem. Eur. J.* **2017**, *23,* 9022–9025. e) M. Abellán Flos, M. I. García Moreno, C. Ortiz Mellet, J. M. García Fernández, J.-F. Nierengarten, S. P. Vincent, *Chem. Eur. J*. **2016**, *22*, 11450-11460. f) T. M. N. Trinh, M. Holler, J. P. Schneider, M. I. Garcia-Moreno, J. M. Garcia-Fernández, A. Boldlenner, P. Compain, C. Ortiz Mellet, J.-F. Nierengarten, *J. Mater. Chem. B* **2017**, *5*, 6546-6556. g) J.-F. Nierengarten, J. P. Schneider, T. M. N. Trinh, A. Joosten, M. Holler, M. L. Lepage, A. Boldlenner, M. I. Garcia-Moreno, C. Ortiz Mellet, P. Compain, *Chem. Eur. J*. **2018**, *24*, 2483-2492.

[5] a) Y. Brissonnet, C. Ortiz Mellet, S. Morandat, M. I. Garcia-Moreno, D. Deniaud, S. E. Matthews, S. Vidal, S. Šesták, K. El Kirat, S. G. Gouin, *J. Am. Chem. Soc.* **2013**, *135*, 18427-18435. b) S. Mirabella, G. D'Adamio, C. Matassini, A. Goti, S. Delgado, A. Gimeno, I. Robina, A. J. Moreno-Vargas, S. Šesták, J. Jimenez-Barbero, F. Cardona, *Chem. Eur. J.* **2017**, *23,* 14585-14596. c) M. Abellán Flos, M. I. García Moreno, C. Ortiz Mellet, J. M. García Fernández, J.-F. Nierengarten, S. P. Vincent, *Chem. Eur. J*. **2016**, *22*, 11450-11460.

[6] For reviews see: a) P. Compain, A. Bodlenner, *ChemBioChem* **2014**, *15, 1239*-1251; b) S. Gouin, *Chem. Eur. J.* **2014**, *20*, 11616-11628. c) N. Kanfar, E. Bartolami, R. Zelli, A. Marra, J.-Y. Winum, P. Dumy, *Org. Biomol. Chem.* **2015**, *13*, 9894-9906; d) C. Matassini, C. Parmeggiani, F. Cardona, A. Goti, *Tetrahedron Lett* **2016**, *57* 5407-5415. e) C. Ortiz Mellet, J.-F. Nierengarten, J. M. Garcia Fernández, *J. Mater. Chem. B* **2017**, *5*, 6428-6436.

[7] M. L. Lepage, J. P. Schneider, A. Bodlenner, A. Meli, F. De Riccardis, M. Schmitt, C. Tarnus, N.-T. Nguyen-Huynh, Y.-N. Francois, E. Leize-Wagner, C. Birck, A. Cousido-Siah, A. Podjarny, I. Izzo, P. Compain, *Chem. Eur. J.* **2016**, *22*, 5151-5155.

[8] a) B. S. Gnanesh Kumar, G. Pohlentz, M. Schulte, M. Mormann, N. Siva Kumar, *Glycobiology* **2014**, *24*, 252-261. b) P. F. Daniel, B. Winchester, C. D. Warren, *Glycobiology* **1994**, *4*, 551-566. c) S. M. Snaith, *Biochem. J.* **1975**, *147*, 83–90.

[9] P. E. Goss, C. L. Reid, D. Bailey, J. W. Dennis, *Clin. Cancer Res.* **1997**, *3*, 1077-1086.

[10] P. Heikinheimo, R. Helland, H. K. Leiros, I. Leiros, S. Karlsen, G. Evjen, R. Ravelli, G. Schoehn, R. Ruigrok, O. K. Tollersrud, S. McSweeney, E. Hough, *J. Mol. Biol.* **2003**, *327*, 631-644

[11] J. M. van den Elsen, D. A. Kuntz, D. R. Rose, *EMBO J* **2001**, *20*, 3008-3017.

[12] S. Howard, S. He, S. G. Withers, *J. Biol. Chem.* **1998**, *273*, 2067-2072.

[13] G. Davies, B. Henrissat, *Structure* **1995**, *3*, 853-859.

[14] P. Emsley, K. Cowtan, *Acta Crystallogr D Biol Crystallogr* **2004**, *60*, 2126-2132.

[15] P. D. Adams, P. V. Afonine, G. Bunkóczi, V. B. Chen, N. Echols, J. J. Headd, L. W. Hung, S. Jain, G. J. Kapral, R. W. Grosse Kunstleve, A. J. McCoy, N. W. Moriarty, R. D. Oeffner, R. J. Read, D. C. Richardson, J. S. Richardson, T. C. Terwilliger, P. H. Zwart, *Methods* **2011**, *55*, 94-106.

[16] V. Wittmann, R. J. Pieters, *Chem. Soc. Rev.* **2013**, *42*, 4492-4503.

[17] a) J. E. Gestwicki, C. W. Cairo, L. E. Strong, K. A. Oetjen, L. L. Kiessling, *J. Am. Chem. Soc.* **2002**, *124*, 14922-14933. b) L. L. Kiessling, J. E. Gestwicki, L. E. Strong, *Angew. Chem. Int. Ed.* **2006**, *4*5, 2348–2368.